Journal of Applied Polymer Science

Structure and Thermomechanical Properties of Stretched Cellulose Films

Jae-Woo Kim,[1] Sunkyu Park,[1,2] David P. Harper,[1] Timothy G. Rials[1]
[1]Center for Renewable Carbon, University of Tennessee, Knoxville, Tennessee 37996
[2]Department of Forest Biomaterials, North Carolina State University, Raleigh, North Carolina 27695
Correspondence to: S. Park (E-mail: sunkyu_park@ncsu.edu)

ABSTRACT: Regenerated and stretched cellulose films were investigated for structure and thermomechanical properties as a potential packaging material. Cellulose films were cast from lithium chloride/*N, N*-dimethylacetamide and were stretched up to 30% in a dynamic mechanical analyzer sample holder. Wide-angle X-ray diffraction analysis indicated that the orientation factor was significantly increased due to stretching. In addition, the stretched films have a higher resistance to the thermal decomposition from thermo gravimetric analysis. The increased orientation of cellulose crystalline structure by the stretching process also increased the storage modulus of cellulose films characterized by dynamic mechanical analysis, which suggest that mechanical properties of cellulose films could be tuned during the stretching process. The $\alpha_2$and α_1 relaxations were found at 240 and 300°C, respectively, which are attributed to the micro-Brownian motion of segments in amorphous region, and activation energies for relaxations were determined with the stretching levels. © 2012 Wiley Periodicals, Inc. J. Appl. Polym. Sci. 000: 000–000, 2012

KEYWORDS: cellulose; stretching; orientation; thermomechanical properties; α-relaxation

Received 25 February 2012; accepted 3 June 2012; published online
DOI: 10.1002/app.38149

INTRODUCTION

Packaging is one of the largest growing industries. The size of the packaging market in the United State is estimated to be $100 billion, and 70% is attributed to food and beverage packaging. Most packaging materials are currently petroleum-derived plastics, which are inexpensive and versatile. However, the growing environmental concern and possible toxic nature of plastics are making a trend for biobased materials due to several reasons, which include: (1) recycling nature of the materials, (2) limited landfill space, (3) government regulation on environment issues, (4) rising petroleum costs, and (5) growing customer's needs that packaging materials be more natural. Many biodegradable and renewable resources have been investigated for packaging applications and used including polysaccharides (starch, cellulose, chitosan, etc.), proteins (casein, soy, etc.), and lipids (fats, waxes, etc.).[1] For example, cellulose film has been used for sausage packaging, and starch container has been used for a vegetable case. As a food packaging material, cellulose films are subjected to a wide range of thermal conditions, freezing to cooking, where it must maintain mechanical and barrier integrity for the safety of the consumer. Further, the films may be subjected to dynamic loading conditions such as in stuffing of cellulose sausage casings. Cellulose displays a wide range of important properties that are greatly influenced by the conformation of cellulose chains in the material. The most common method to enhance the mechanical properties of cellulose film is drawing. The drawing treatment improves the orientation of cellulose chains and crystallinity in the drawn cellulose.[2,3] However, little has been known for the thermal and thermomechanical properties of drawn cellulose film. As demand grows for biobased polymers, a better understanding of the relationship between crystal orientation and thermomechanical properties become necessary. In this study, regenerated cellulose films were stretched, and their structural, thermal, and thermomechanical properties were investigated.

MATERIALS AND METHODS

Cellulose Film Preparation

Microcrystalline cellulose (Avicel PH-101 from Sigma–Aldrich, St. Louis, MO) was used as a starting material. To dissolve cellulose, cellulose powder has to be activated by swelling the cellulose followed by solvent exchanges. Cellulose was immersed in water overnight and filtered to remove the water. Then, the cellulose was immersed in methanol and filtered three times in 3 h. After the methanol exchange, the cellulose was immersed in *N, N*-dimethylacetamide (DMAc) and filtered. This step was also repeated three times in 3 h. In parallel, 8 wt % lithium chloride

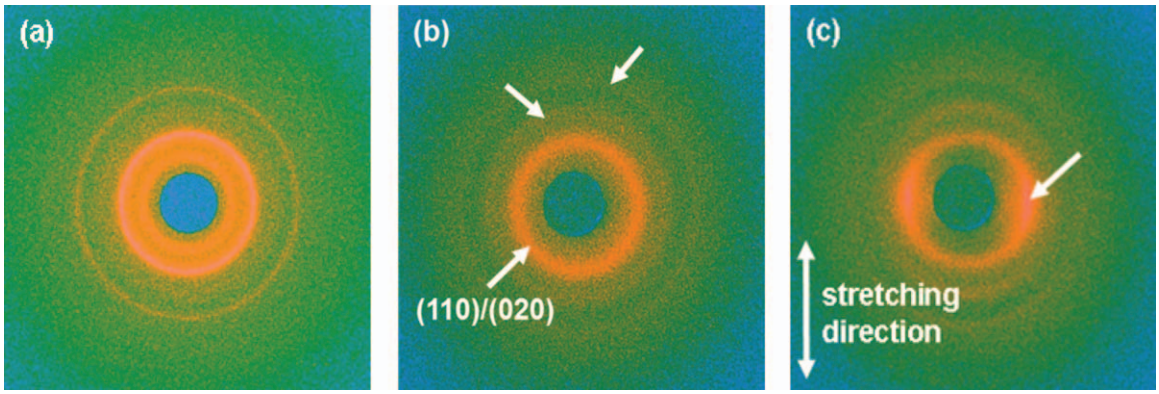

Figure 1. WAXD patterns for (a) microcrystalline cellulose powder, (b) unstretched cellulose film, and (c) 30% stretched cellulose film. Arrow in (c) indicates the effect of stretching process on cellulose structure. Stretching direction is indicated in figure. [Color figure can be viewed in the online issue, which is available at wileyonlinelibrary.com.]

(LiCl) in DMAc was prepared as a solvent system. Finally, activated cellulose was dissolved in LiCl/DMAc at 2 wt % concentration. The solution was stirred at room temperature until the complete dissolution of cellulose. Dissolved cellulose solution was filtered to remove any insoluble portion using syringe filter (Whatman PTFE filter with Polypropylene housing) having a pore size of 0.45 μm.

Cellulose films from LiCl/DMAc were prepared by slow precipitation. The solution was poured into a glass Petri dish having a 10-cm diameter and left at an ambient atmosphere. In this manner, DMAc was slowly evaporated, and water vapor diffused into the solution, precipitating the cellulose. The precipitation continued until a disk-shaped transparent gel was formed. The duration of the casting process varied depending on atmospheric conditions such as relative humidity, temperature, and air circulation from 24 to 72 h. The gel was then washed with water for 7 days to remove remaining LiCl and DMAc and then dried in an oven at 60°C. To evenly distribute drying stress over the entire film and prevent the film shrinkage during drying, the gelatinous cellulose was placed onto the same size of plastic plate and gently clamped using binder clips. The final thicknesses of dried films were fairly uniform measuring around 45 μm. They were further cut into strips of 50-mm length and 5-mm width.

Stretching of Cellulose Film

To introduce preferred orientation, cellulose films were immersed in water overnight, and the fully swollen cellulose films were mounted to dynamic mechanical analyzer (DMA) machine (Pyris Diamond DMA from PerkinElmer, Waltham, MA). Films were stretched uniaxially at room temperature to the desired stretching ratios, which are 0, 10, 20, and 30%. These correspond to 2.0, 2.2, 2.4, and 2.6 mm in length. Stretched films were completely dried in the DMA to prevent unwanted shrinkage, if the film was released.

Wide-Angle X-Ray Diffraction

To determine the crystalline structure of the cellulose films, wide-angle X-ray diffraction (WAXD; Molecular Metrology WAXD system) was used. This is a typical pin-hole system equipped with a Bede X-ray generator (Bede Scientific Incorporated) operated at a voltage of 45 kV and a current of 0.66 mA. The system has a double focusing mirror to enhance the intensity and produces monochromatic CuKα radiation having a wavelength of 0.1542 nm. Samples were exposed in X-ray for 30 min to obtain X-ray diffraction patterns from 5 to 70° of 2θ scattering angle on Fuji image plate. The sample-to-plate distance was 36.52 mm. The diffracted 2D WAXD pattern was scanned in a Fuji BAS-1800II image analyzer, and the resultant image was then converted to 1D intensity plot using X-ray analysis software (POLAR, Stony Brook Technology and Applied Research).

The 1D intensity profile was peak-fitted to separate amorphous peak and crystalline peaks using curve-fitting software (PeakFit, Systat Software, www.systat.com). The center of the amorphous peak was predetermined to be 19.1° of 2θ based on WAXD data using the amorphous cellulose powder provided from USDA-FS. Amorphous powder was ball-milled for 120 min, and no crystalline peak was observed. Clear reflection band from (1 1 0)/(0 2 0) plane is identified in Figure 1(b). A peak fitting program (PeakFit, Systat Software, www.systat.com) was used to extract individual crystalline peaks from the diffraction intensity profiles, assuming Gaussian functions for each peak and a broad amorphous halo.[4,5] Apparent crystal size in the perpendicular to the (1 1 0)/(0 2 0) plane was determined using Scherrer equation, eq. (1).

$$L = \frac{k \cdot \lambda}{\beta \cdot \cos\theta} \tag{1}$$

where k is the Scherrer constant (0.94),[6] λ is the X-ray wavelength (0.1542 nm), β is the full-width at half-maximum, and θ is the Bragg angle. Crystal orientation factor, f_c, in cellulose films was calculated using the Herman's equation, eq. (2).

$$f_c = 1 - \frac{3}{2}\left\langle \frac{\int_0^{\pi/2} I(\phi)\sin^3\phi d\phi}{\int_0^{\pi/2} I(\phi)\sin\phi d\phi} \right\rangle \tag{2}$$

where ϕ is the azimuthal angle and $I(\phi)$ is the intensity along the (1 1 0)/(0 2 0) reflection. Maximum orientation is found when $f_c = 1$ and $f_c = 0$ indicates random orientation.

Thermal and Thermomechanical Analysis

Thermal properties such as degradation and glass transition temperature of cellulose films were investigated using thermogravimetry (TG, PerkinElmer Pyris 1 TGA) and differential scanning calorimetry (DSC, PerkinElmer Diamond DSC). TG was operated

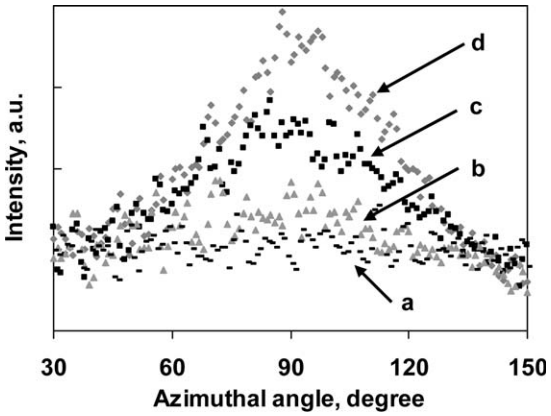

Figure 2. Intensity of azimuthal reflection for (a) unstretched, (b) 10% stretched, (c) 20% stretched, and (d) 30% stretched cellulose films. Integration was performed at the plane (1 1 0)/(0 2 0), which was 19.8° ± 1°, with the caking angle of 30–150°.

from 30 to 700°C with about 5 mg of sample, while DSC was operated from 30 to 400°C with the sample size of about 2 mg. Both TG and DSC were operated at the heating rate of 5°C/min under the nitrogen flow.

Thermomechanical properties were determined using DMA (PerkinElmer Pyris Diamond DMA) with sinusoidal tension mode at the heating rate of 5°C/min. With measurements at the various frequencies (1, 2, 4, 10, 20, and 40 Hz), the activation energy (AE, kJ/mol) of phase transitions was calculated from the Arrhenius rate relationship, eq. (3).

$$\log f = -(AE/RT) \quad (3)$$

Where f is the frequency (Hz), R is the gas constant (8.314 J/K mol), and T is the temperature (K).

RESULTS AND DISCUSSION

Stretching of Cellulose Films

Cellulose films were slowly cast in Petri dishes by the evaporation of DMAc and the diffusion of water vapor. After the casting and washing, the cellulose films were highly swollen gels containing about 95% of water in mass. During the drying process, intermolecular hydrogen bonds are formed, and drawability is greatly reduced by these bonds. A previous study reported that the dissociation energy for about 20 hydrogen bonds is assumed to correspond to that of a covalent bond.[7] Thus, the ideal methodology is to stretch the films in never-dried wet state. Although it was reported that highly water-swollen gel state could be stretched in a "manual stretching device," the never-dried cellulose films were too fragile to clamp during the stretching process.[2] Instead, once dried films were immersed in water overnight and stretched in a DMA sample holder. Gindl et al. also used once dried films and stretched the samples in tensile test machine.[3] For this reason, maximum drawability was found to be 130% in this study, which was lower than previously reported value of 200% for never-dried wet films.[2]

Another reason for the low drawability is the restrained drying of cellulose films. To prevent unwanted shrinkage during the air or oven drying of water-swollen films, a clamping device was used. In this way, drying stress could be evenly distributed. In addition, the surface of the dried films appeared much smoother than air-dried film. This greatly contributes to generating reproducible and less noisy data, which is critical to distinguish weak secondary transitions.

Structural Changes in Stretched Cellulose Films

WAXD patterns of unstretched and 30% stretched cellulose films are shown in Figure 1. For the unstretched film [Figure 1(b)], a broad diffuse ring appeared at 19.8° of 2θ angle. Compared with the diffraction pattern of microcrystalline cellulose powder in Figure 1(a), regenerated cellulose exhibits the cellulose II structure, indicating that cellulose I structure in powder was completely converted to cellulose II structure. This characteristic peak for cellulose II structure was analyzed to consist of two crystalline peaks, which were assigned the reflection plane of (1 1 0) and (0 2 0) from synchrotron X-ray experiments.[8] For the samples in this study, however, overlapping peaks of (1 1 0) and (0 2 0) are not sharp enough to separate. This is attributed to the separation power of X-ray source and the amorphous nature of cellulose films cast from LiCl/DMAc comparing to the cellulose fibers. Thus, this peak is assigned to (1 1 0)/(0 2 0) in this study, which can be found in many other studies.[2,9] In addition, relatively small peaks are found at 28.0° and 35.5°, which were identified with arrows.

With the increasing stretching ratio, the higher degree of orientation is observed. Figure 1(c) shows that the image pattern greatly altered when the film was stretched at 30%. The diffuse ring became thinner along with the meridional direction (stretching direction) and thicker at the equatorial direction [perpendicular to stretching direction, see an arrow in Figure 1(c)]. The effect of stretching on the orientation of film structure was clearly demonstrated, when the diffused pattern is plotted azimuthal angle versus intensity in Figure 2. Integrated intensity at the plane (1 1 0)/(0 2 0), which was 19.8° ± 1°, clearly showed the effect of stretching process.

To calculate crystallinity and crystal size, 1D intensity profile was obtained by 360° integration of the 2D WAXD pattern with the 2θ angle of 5–40°. Assuming crystalline peaks and amorphous peak as Gaussian curves, overlapped peaks were successfully separated with high R^2 and F values as shown in Table I, which were greater than 0.997 and 6000 for all cases. Crystallinity index of unstretched film was 35.5% and tends to slightly increase with the stretching ratio (9.6% increment from 35.5 to 38.9). This is consistent with a general concept that the crystallinity of semicrystalline polymers can be increased by stretching due to the rearrangement of the polymer chains to the stretching direction. For the crystal size, 1.7% decrease from 2.36 to 2.32 nm is not considered a significant change, considering broad and scattered X-ray data.

Although the changes in crystallinity and crystal size were small and negligible, the orientation factor shows considerable changes upon the stretching process. Crystalline orientation factor, f_c, were found 0.00, 0.05, 0.09, and 0.13 for unstretched, 10, 20, and 30% stretched cellulose films, respectively, which are consistent with other study.[3] This indicates that crystalline

Table I. Structural Properties of Cellulose Films from WAXD Analysis

Cellulose films	Crystallinity index (%)	Crystal size (nm)	Orientation factor f_c	R^{2a}	F^b
Unstretched	35.5	2.36	0.00	0.998	7037
10% stretched	37.0	2.35	0.05	0.998	7987
20% stretched	38.8	2.33	0.09	0.997	6235
30% stretched	38.9	2.32	0.13	0.998	8806

[a]Coefficients of determination for fitting, [b]*F*-statistic for fitting.

cellulose that is associated with the amorphous region become preferentially oriented to the stretching direction.

Thermal Analysis of Stretched Cellulose Films

All cellulose films have the similar decomposition temperatures of about 310°C as shown in Figure 3. It is well known that cellulose has a high thermal stability due to the intramolecular and intermolecular hydrogen bonds. Interesting observation was the rate of decomposition. When the weight loss derivatives of cellulose films are plotted in Figure 4, unstretched film has a higher value than stretched films, indicating faster decomposition. In other words, stretched films have a higher resistance to thermal decomposition. Exact volume of film or void volume in film was not measured in this study, but it was noticed that the width and thickness of films were reduced with the stretching process, resulting in tightly packed amorphous regions. Therefore, this packed structure is considered to impact the slow decomposition of stretched films.

To determine the glass transition temperature of cellulose films, a step scan mode was used, because conventional DSC operation is not able to distinguish between reversible and nonreversible heat flow, such as decomposition of cellulose. Step scan mode utilizes the heating of sample over the small temperature increments with the holding for a short time interval. The glass transition temperatures of cellulose films were found at 300°C regardless of stretching levels in Figure 5, which were slightly lower than the thermal decomposition characterized by TG.

Thermomechanical Properties of Stretched Cellulose Films

DMA is generally recognized to be sensitive to molecular motions and useful for evaluating subtle transitions occurred in polymeric system.[10] Figure 6 shows that the dependence of storage modulus (E') on temperature for the cellulose films. The modulus decreases gradually with increasing temperature until a sharp decrease, which is attributed to the thermal decomposition. The modulus value of unstretched film was found about 3 $\times$ 10^9 Pa, which is slightly higher than other work of 1–2 $\times$ 10^9 Pa, when it was prepared from cotton linter dissolved in NaOH/urea.[11] The modulus of the stretched film increases with the stretching level indicating higher stiffness of stretched films along the stretched direction. It is worth noting that the difference in modulus becomes smaller with the increased temperature, and no noticeable difference is observed after the glass transition temperature, 300°C. Although tensile strength was not measured in this study, tensile strength increased with the stretching process of regenerated cellulose films[6] and regenerated cellulose fibers.[12] The hypothesis for the increased mechanical properties has been proposed that intermolecular hydrogen bonds among adjacent cellulose chains in noncrystalline regions are not dissociated, but remain the bonds during the stretching process.[2] In this way, the crystallinity index did not show any significant change with the stretching, whereas the mechanical properties have been improved due to the high orientation of the molecular chains. Another explanation might be due to the rearrangement of intermolecular hydrogen bonds between glucan chains. During the stretching process, some of intermolecular hydrogen bonds could be broken and rebonded to different locations at the stretched condition. Therefore, mechanical properties are increased to the stretching direction. In addition, tightly packed amorphous structure is believed to contribute higher mechanical properties in films. Crystallinity might not

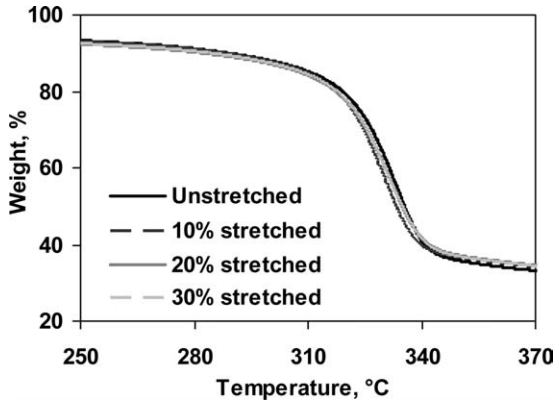

Figure 3. Thermal decomposition of cellulose films in TG with nitrogen purge.

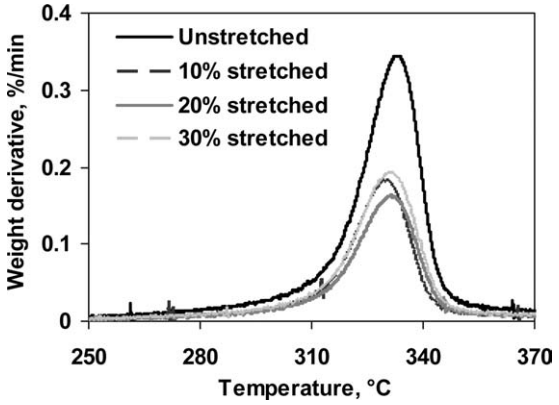

Figure 4. Weight derivative of thermal decomposition of cellulose films. Unstretched film has higher value than stretched films.

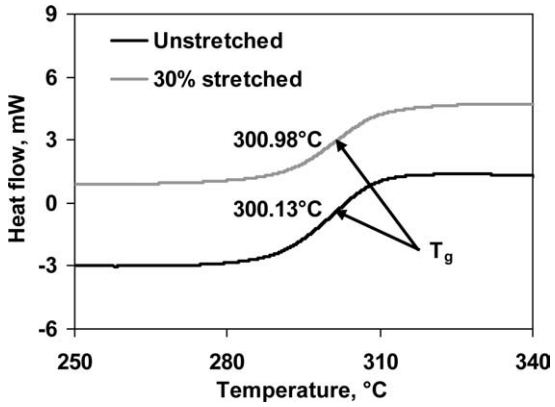

Figure 5. Glass transition temperature of cellulose films characterized by step scan DSC operation.

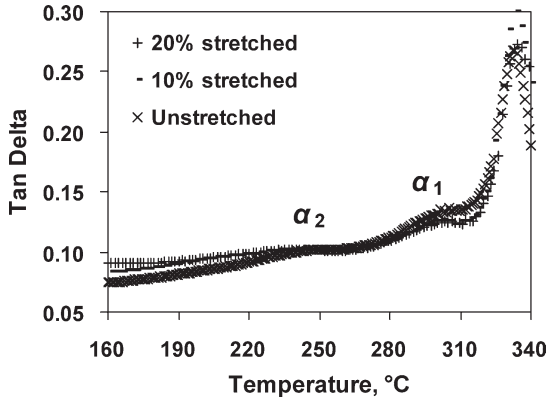

Figure 7. Temperature dependence of mechanical loss factor (tan δ) for the cellulose films. Mechanical relaxations are observed as α_2 and α_1 relaxations.

be affected largely, because rearrangement can occur at localized points and is not enough to impart crystal growth.

The dependence of loss factor is plotted versus temperature in Figure 7. In general, the relaxation peaks are assigned to the molecular motions of polymeric system. Bradley and Carr[13] reported four different transitions of cellophane film, which were γ, β, α_2, and α_1 relaxations. The γ and β relaxations of cellulose have been studied extensively with dielectric spectroscopy.[14,15] The γ relaxation was found about -120°C and explained to be associated with the rotation of primary hydroxyl groups.[16] The β relaxation was observed about -50°C, and it was proposed that this process was associated with the main chain segments, not side-group reorientation.[17] However, the α_2 relaxation has been relatively less studied due to the difficulty of observations. For example, the α_2 relaxation was not observed from the NaOH or NaOH/urea solution casting with cotton linter,[18] viscose rayon,[19] and cuprammonium rayon.[20] In this study, two thermomechanical transitions are clearly observed at 240 and 300°C, which were labeled as α_2 and α_1, respectively. It is noted that the DMA results in this study were less noisy than others due to the cautious preparation of cellulose films including (1) restrained drying that distributes drying stress evenly, (2) DMA stretching that controls the stretching process exactly, and (3) DMA drying that eliminates possible unwanted shrinkage.

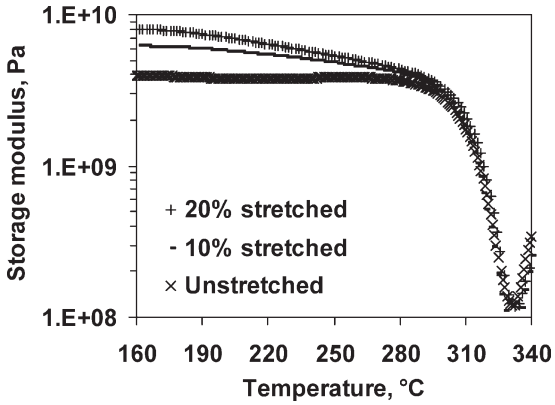

Figure 6. Temperature dependence of storage modulus (E') for the cellulose films. Higher modulus is observed with the stretching process of films.

These relaxations are originated from the micro-Brownian motion of segments in amorphous region, which is dominated by the segment environment such as the density of intermolecular and intramolecular hydrogen bonding. Based on DSC results in Figure 5, the α_1 relaxation is considered as glass transition temperature, which is the physical property of amorphous material from glassy state to rubbery state. The nature of the α_2 relaxation is rather unclear due to the complexity of different structural levels of cellulose. However, it has been proposed that the α_2 relaxation corresponds to the amorphous region of moderately developed intramolecular and intermolecular hydrogen bonds, whereas the α_1 relaxation corresponds to the amorphous region of cellulose chains, in which intramolecular and intermolecular hydrogen bonds are strongly and densely formed.[21,22] The broad and weak α_2 relaxation was observed at 240°C in Figure 7, and this is consistent with results found from other research at 223°C,[11] 240–290°C,[22] and 237°C.[21]

The relaxation peaks, α_2 and α_1, shift to higher temperatures with increasing frequency as expected for any thermally activated relaxation process. Within the frequency range (1–40 Hz) used in this study, the frequency dependence of the two peak temperatures is plotted in Figures 8 and 9. The calculated activation energies for stretched cellulose films based on the Arrhenius equation are summarized in Table II. The regression coefficients (R^2) of Arrhenius plots were reasonably high. In general, the AE largely depends on moisture levels in most case, but cellulose films in this study were completely dried sample. The activation energies varied within 360–416 kJ/mol for α_2 relaxation and 229–258 kJ/mol for α_1 relaxation. The AE of the α_2 relaxation was reported 209–289 kJ/mol[21] and 314 kJ/mol[13] for different types of regenerated celluloses. The AE of the α_2 relaxation showed an increase with the stretching process. This increased AE is indicative of an increase in the interaction of

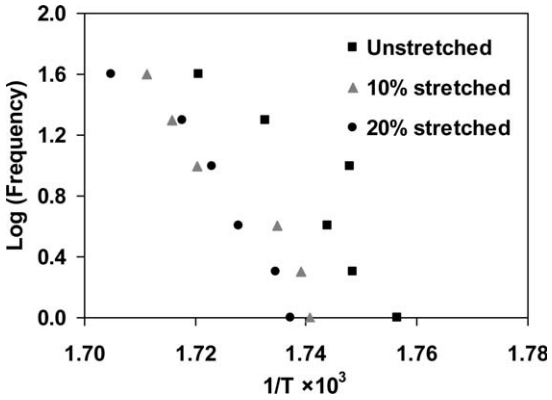

Figure 8. Arrhenius plot of log frequency versus $1/T$ for the α_1 relaxation.

glycosidic units that requires more cooperative motions for relaxation due to tightly packed amorphous regions. However, an increase in the orientation of cellulose crystal results in a slight decreased trend for the α_1 relaxation. A similar result has been observed in molecular modeling studies whereas orientation increases, there is a decrease in the interaction between cellulose chains.[23] Stretching the films can fix the structure in a position not optimal for crystallization but increases cellulose chain packing density in amorphous regions.

CONCLUSIONS

Structure and thermomechanical properties of cellulose films as a potential packaging material were investigated with the stretching levels. Cellulose films were cast from lithium chloride/DMAc and were stretched up to 30% in a DMA sample holder. From the WAXD analysis, it was found that orientation factor was considerably increased while the changes in crystallinity and crystal size were small and negligible. The rate of decomposition of cellulose films was analyzed using TG that the stretched films have a higher resistance to the thermal decomposition. The increased orientation of cellulose crystalline structure by the stretching process also increased the storage modulus of cellulose films characterized by dynamic mechanical analysis. It is considered due to the tightly packed amorphous

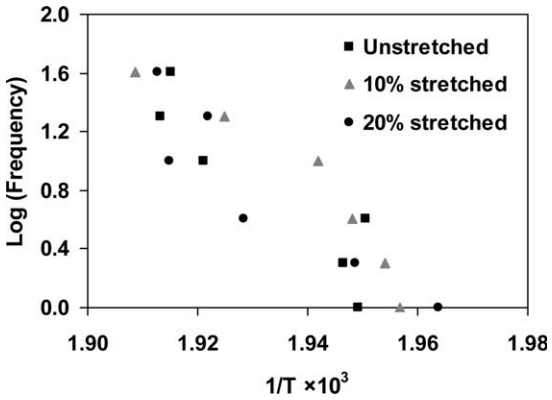

Figure 9. Arrhenius plot of log frequency versus $1/T$ for the α_2 relaxation.

Table II. Apparent AE of the α_2 and α_1 Relaxations from Arrhenius Plots (Figures 8 and 9) Applied to Multifrequency DMA Data

Cellulose films	AE for α_2 relaxation (kJ/mol)	R^2 for α_2 relaxation	AE for α_1 relaxation (kJ/mol)	R^2 for α_1 relaxation
Unstretched	360	0.828	258	0.828
10% stretched	391	0.904	257	0.962
20% stretched	416	0.845	229	0.945

structure during glucan chain rearrangement induced by stretching process. The α_1 relaxation at 300°C by the DMA experiment was confirmed as a glass transition temperature by the DSC operation. Interesting observation was thermomechanical transitions found at 240°C. The existence of this α_2 relaxation could be explained by the moderately developed intramolecular and intermolecular hydrogen bonds in cellulose amorphous region. The results of this study suggest that mechanical properties of cellulose films could be tuned during the stretching process. In addition, two different transitions, α_2 and α_1 relaxations, represent the complex nature of cellulose structure, in which further studies are required for better understanding.

ACKNOWLEDGMENTS

The authors thank Dr. Umesh Agarwal at Forest Products Laboratory (Madison, WI) for the amorphous cellulose sample.

REFERENCES

1. Robertson, G. L. Food Packaging Materials; CRC Press: Boca Raton, **2006;** 152 pp.
2. Togawa, E.; Kondo, T. *J. Polym. Sci. B: Polym. Phys.* **1999,** *37*, 451.
3. Gindl, W.; Martinschitz, K. J.; Boesecke, P.; Keckes, J. *Biomacromolecules* **2006,** *7*, 3146.
4. Park, S.; Johnson, D. K.; Ishizawa, C. I.; Parilla, P.; and Davis, M. F. *Cellulose* **2009,** *16*, 641.
5. Park, S.; Himmel, M. E.; Baker, J. O.; Johnson, D. K. *Biotechnol. Biofuels* **2010,** *3*, 1.
6. Oh, S. Y.; Yoo, D. I.; Shin, Y.; Kim, H. C.; Kim, H. Y.; Chung, Y. S.; Park, W. H.; Youk, J. H. *Carbohydr. Res.* **2005,** *340*, 2376.
7. Postema, A. R.; Smith, P.; English, A. D. *Polym. Commun.* **1990,** *31*, 444.
8. Chen, X.; Burger, C.; Fang, D.; Ruan, D.; Zhang, L.; Hsiao, B. S.; Chu, B. *Polymer* **2006,** *47*, 2839.
9. Hiraishi, M.; Igarashi, K.; Kimura, S.; Wada, M.; Kitaoka, M.; Samejima, M. *Carbohydr. Res.* **2009,** *344*, 2468.
10. Lazaridou, A.; Biliaderis, C. G.; Kontogiorgos, V. *Carbohydr. Polym.* **2003,** *52*, 151.
11. Lu, Y.; Zhang, L.; Xiao, P. *Polym. Degrad. Stab.* **2004,** *86*, 51.

12. Kong, K.; Eichhorn, S. J. *Polymer* **2005,** *46*, 6380.
13. Bradley, S. A.; Carr, S. H. *J. Polym. Sci. B: Polym. Phys.* **1976,** *14*, 111.
14. Nishinari, K.; Shibuya, N.; Kainuma, K. *Makromol. Chem.—Macromol. Chem. Phys.* **1985,** *186*, 433.
15. Hongo, T.; Yamane, C.; Saito, M.; Okajima, K. *Polym. J.* **1996,** *28*, 769.
16. Montès, H.; Mazeau, K.; Cavaillé, J. Y. *Macromolecules* **1997,** *30*, 6977.
17. Einfeldt, J.; Meißner, D.; Kwasniewski, A. *Cellulose* **2004,** *11*, 137.
18. Ruan, D.; Huang, Q.; Zhang, L. *Macromol. Mater. Eng.* **2005,** *290*, 1017.
19. Ruan, D.; Zhang, L.; Zhang, Z.; Xia, X. *J. Polym. Sci. B: Polym. Phys.* **2004,** *42*, 367.
20. Yang, G.; Miyamoto, H.; Yamane, C.; Okajima, K. *Polym. J.* **2007,** *39*, 34.
21. Manabe, S.; Iwata, M.; Kamide, K. *Polym. J.* **1986,** *18*, 1.
22. Yamane, C.; Mori, M.; Saito, M.; Okajima, K. *Polym. J.* **1996,** *28*, 1039.
23. Chen, W.; Lickfield, G. C.; Yang, C. Q. *Polymer* **2004,** *45*, 1063.